Development of a TCR-like antibody and chimeric antigen receptor against NY-ESO-1/HLA-A2 for cancer immunotherapy

Xin Liu,[1,2,3] Yixiang Xu,[4] Wei Xiong [ID],[4] Bingnan Yin,[1,2] Yuqian Huang,[2,5] Junjun Chu,[1,2] Changsheng Xing,[1,2] Chen Qian,[1,2] Yang Du,[1,2] Tianhao Duan,[1,2] Helen Y Wang,[1,2] Ningyan Zhang,[4] John S. Yu,[6] Zhiqiang An,[4] Rongfu Wang [ID] [1,2,3]

ABSTRACT

Background The current therapeutic antibodies and chimeric antigen receptor (CAR) T cells are capable of recognizing surface antigens, but not of intracellular proteins, thus limiting the target coverage for drug development. To mimic the feature of T-cell receptor (TCR) that recognizes the complex of major histocompatibility class I and peptide on the cell surface derived from the processed intracellular antigen, we used NY-ESO-1, a cancer-testis antigen, to develop a TCR-like fully human IgG1 antibody and its derivative, CAR-T cells, for cancer immunotherapy.

Methods Human single-chain variable antibody fragment (scFv) phage library ($\sim 10^{11}$) was screened against HLA-A2/NY-ESO-1 (peptide 157–165) complex to obtain target-specific antibodies. The specificity and affinity of those antibodies were characterized by flow cytometry, ELISA, biolayer interferometry, and confocal imaging. The biological functions of CAR-T cells were evaluated against target tumor cells in vitro. In vivo antitumor activity was investigated in a triple-negative breast cancer (TNBC) model and primary melanoma tumor model in immunocompromised mice.

Results Monoclonal antibody 2D2 identified from phage-displayed library specifically bound to NY-ESO-1$_{157-165}$ in the context of human leukocyte antigen HLA-A*02:01 but not to non-A2 or NY-ESO-1 negative cells. The second-generation CAR-T cells engineered from 2D2 specifically recognized and eliminated A2+/NY-ESO-1+tumor cells in vitro, inhibited tumor growth, and prolonged the overall survival of mice in TNBC and primary melanoma tumor model in vivo.

Conclusions This study showed the specificity of the antibody identified from human scFv phage library and demonstrated the potential antitumor activity by TCR-like CAR-T cells both in vitro and in vivo, warranting further preclinical and clinical evaluation of the TCR-like antibody in patients. The generation of TCR-like antibody and its CAR-T cells provides the state-of-the-art platform and proof-of-concept validation to broaden the scope of target antigen recognition and sheds light on the development of novel therapeutics for cancer immunotherapy.

BACKGROUND

Immunotherapies of therapeutic monoclonal antibodies are emerging as a major

Key messages

What is already known on this topic
► NY-ESO-1 is one of the best and immunogenic cancer antigens for immunotherapy in solid tumors. However, there are no TCR-like antibody or CAR-T cells specifically targeting intracellular NY-ESO-1 protein or its complex with HLA-A2 molecules because the reported TCR-like antibody or CAR-T cells targeting HLA-A2/NY-ESO-1 complexes show off-target recognition against HLA-A2 molecules.

What this study adds
► This study has identified a novel HLA-A2/NY-ESO-1 complex-specific TCR-like antibody. Furthermore, TCR-like antibody-based CAR-T cells demonstrated potent antitumor response, without evident toxicity.

How this study might affect research, practice or policy
► This study may facilitate the development of novel cancer immunotherapy using HLA-A2/NY-ESO-1 complex-specific TCR-like antibodies and/or its derived CAR-T cells.

development to cancer treatment.[1] Similarly, chimeric antigen receptor (CAR) engineered T cells show impressive clinical benefits in leukemia and lymphoma.[2 3] However, due to a paucity of ideal and targetable tumor-associated antigens expressed on tumor surface, the application of CAR-T therapy has been severely limited in patients with solid cancers.[4–6] Despite the limited surface antigens, there are a large number of intracellular antigens that could serve as cancer-specific immune targets, which include cancer-testis antigens and mutation-derived neoantigens.[7 8]

Cancer-testis antigens are considered promising target antigens for cancer immunotherapy.[8 9] New York Esophageal Squamous Cell Carcinoma-1 (NY-ESO-1) is not

expressed in normal tissues with exception of the testis but is highly expressed in many types of cancer, including melanoma, sarcoma, and multiple myeloma.[10–13] Others and our studies show that NY-ESO-1 is one of the most immunogenic antigens recognized by T cells derived from patients with cancer.[14–21] Recent studies show that immunotherapy using HLA-A2-restricted NY-ESO-1-specific T cell receptor (A2-ESO-1 TCR) engineered T cells led to a 55% clinical response rate in metastatic synovial sarcoma and melanoma and 80% in myeloma without toxicity.[22–24] Furthermore, TCR-like antibody approaches have been developed to show that, like TCRs, antibodies could also recognize peptide/major histocompatibility complex (MHC) complexes on the cancer cell surface, thus opening the new opportunity to target intracellular cancer antigens that are processed and presented onto the cell surface by MHC molecules. Antigen-specific antibodies could be screened from synthetic human single-chain variable antibody fragment (scFv), Fab phage library, or hybridomas generated from immunized animals such as mice.[25 26] Those TCR-like monoclonal antibodies (mAbs) displayed highly specific binding affinity and killing ability in vitro and in vivo.[27] Moreover, mAbs can be readily further modified and optimized, and derivatives from TCR-like antibodies, such as antibody-drug conjugates, bispecific T cells engagers, and CAR-T cells have yielded impressive results.[28–33]

Here, we report the development of a TCR-like antibody mAb 2D2 that recognizes HLA-A2+/NY-ESO-1$_{157-165}$ peptide complexes and tumor cells with high specificity. CAR construct derived from scFv of 2D2 demonstrates its ability to eliminate target tumor cells. This is the first successful report of CAR-T cells targeting NY-ESO-1, with both in vitro and in vivo antitumor activity and specificity. Collectively, our data highlights a novel CAR-T technology and a new strategic application to immunotherapy.

METHODS
Animal
NSG mice 6–8 weeks of age (NOD.Cg-Prkdcscid Il2rgtm1Wjl/SzJ) and NSG-A2 mice aged 6–8 weeks (NOD.Cg-Prkdcscid Il2rgtm1Wjl Tg(HLA-A/H2-D/B2M)1Dvs/SzJ) were purchased from Jackson Laboratory (cat. no. 005557, cat. no. 014570) or bred in the animal facility at Houston Methodist Research Institute or University of Southern California. All procedures have been approved by Houston Methodist Research Institute Animal Care and Use Committee and University of Southern California Animal Care and Use Committee (IACUC). In the TNBC model, female NSG mice were used, and in the primary melanoma model, male NSG mice were used. Mice were housed under a 12:12 light:dark cycle, and all the facilities are accredited by the Association for Assessment and Accreditation of Laboratory Animal Care International. No a priori sample size calculation nor data exclusion was made in all experiments. Mice were randomly distributed into control group and treatment group. Tumor cells

and T cells injections were done by investigator A, and tumor size was measured by investigator B. Mice were sacrificed when reaching endpoint that the diameter of tumor approaches 2 cm or other endpoints listed in the protocol.

For the TNBC model, female mice were first challenged with 2 million MDA-MB-231-ESO tumor cells at fat pad. On day 4, mice were intravenously treated with 10 million control T cells or 2D2-CAR T cells suspended in 200 µL PBS, respectively, followed by three doses of 50,000 IU recombinant human IL-2 intraperitoneally. Mice were closely monitored, and tumor volume was measured via vernier caliper at indicated days.

For the melanoma model, 2 million Mel 1558 tumor cells were subcutaneously implanted at right flank of male NSG mice. A total of 2.5 million 2D2-CAR T cells were injected on day 4 followed by 50,000 IU rhIL-2 intraperitoneally.

For safety assessment, NSG-A2 mice (n=6) were treated with the same dose used to achieve effective therapy (10 million T cells, intravenous injection). The in vivo toxicity was determined based on the body weight loss and histopathological microscopic evaluation of the major tissues. On day 7, three mice were euthanized by carbon dioxide (CO_2) inhalation, and tissue samples were collected. The remaining three mice were euthanized on day 14 for key tissues collection. Bloods were collected in mini lavender top tubes (Greiner, 450573VET) for complete blood count (CBC), while sera were collected in golden top clot activator serum separation tubes (Greiner, 450571VET) for superchem analysis (Antech Diagnostics).

Cell lines
HEK293T, MDA-MB-231-ESO1, and PC3-A2-ESO1 were cultured in DMEM supplied with 10% inactivated FBS and 100 unit/mL of penicillin and 100 µg/mL of streptomycin. T2 cells, Mel 586, Mel 624 and Mel 1558 were cultured with RPMI-1640 containing 10% inactivated FBS and 100 unit/mL of penicillin and 100 µg/mL of streptomycin. All cells were routinely tested as mycoplasma negative.

Panning of phage-displayed scFv antibody library
Human scFv phage-display antibody library (~10^{11} clones) was constructed in lab.[34] For peptide-MHC complex panning (synthesized by the NIH tetramer facility), an in-solution method was adopted to avoid the disadvantage of the immobilization method that may cause conformational changes of the pMHC complex. Briefly, the scFv phage was blocked with an equal amount of 10% milk for 1 hour at room temperature. One hundred microliters of streptavidin-conjugated Dynabeads M-280 (Thermo Fisher, 11206D) were blocked with 5% milk at room temperature for 1 hour. The first round of negative selection against control biotinylated-pMHC (pp65 peptide/HLA*0201, 200 nM) was mixed with blocked phage and beads. After incubation at room temperature for 1 hour,

beads were pulled down through a magnetic rack, and the deselected phages were transferred to a new tube and incubated with the biotinylated NY-ESO-1/HLA*0201 complex for 1 hour. Mixed with 100 µL streptavidin-conjugated dynabeads and incubated for one more hour. Beads were pulled down and washed quickly with PBST (0.05%) twice, followed by a three-time wash with a 5 min incubation, and then quickly washed with PBS twice. The remaining phages on beads were eluted by adding 200 µL fresh 100 mM TEA with 20 min incubation. The supernatant was transferred to a 50 mL tube and neutralized with 0.5 volume 1 M Tris-HCl (pH 7.5). Next, 10 mL fresh prepared TG1 cells (OD600: 0.5–0.8) were added to the neutralized phage and incubated at 37°C for 1 hour at 250 rpm. The infected TG1 cells were inoculated on a 2xYTA plate with antibiotics and incubated at 30°C overnight. The input and output phage were tittered, and the enrichment ratio was calculated. The panning process was repeated three rounds, with decreased biotinylated NY-ESO-1/HLA*0201 complex concentration (200 nM-50 nM-10nM).

Phage ELISA

After three rounds of phage panning, the output phage-infected TG1 clones were picked by colony picker (Molecular Devices) into 96-well plates and cultured at 775 rpm at 37°C with 80% humidity overnight. Phage ELISA was exactly performed as follows: first, transfer 3 µL overnight cultured bacteria to a new 96-well plate with 120 µL 2xYTAG medium; second, incubate 1.5–2 hours at 37°C at 775 rpm with 80% humidity until OD600 reaches 0.4–0.8; then, add 20 µL/well diluted M13K07 helper phage to obtain a ratio of 10 helper phages: 1 bacterial cell and incubate 1 hour; after that, pellet the bacteria and resuspend with 150 µL/well 2xYTAK medium containing 0.5 mM IPTG and culture at 30°C, 775 rpm with 80% humidity overnight; finally, centrifuge the plates at 2500 g for 20 min and use the supernatants for the ELISA.

ELISA was performed as follows: 96-well high binding plates were coated with 100 µL/well streptavidin (2 µg/mL) overnight at 4°C. The next day, plates were blocked with 5% bovine serum albumin (BSA) and then incubated for 1 hour at room temperature with 100 µL/well NY-ESO-1/HLA-A2 complex (2 µg/mL). Then 100 µL/well supernatants were added and incubated for 1 hour followed by washes three times with phosphate-buffered saline with Tween 20 (PBST) and two times with phosphate-buffered saline (PBS). HRP conjugated anti-M13 IgG (Santa Cruz Biotechnology) was used to detect the remaining phage. TMB was used as the substrate, and OD450 was measured.

Antibody production and purification

Phagemids of positive clones were extracted for DNA sequencing. After sequencing analysis with IMGT, CDR diversity was summarized, and unique combinations of heavy chain and light chain nucleotide sequences were obtained. Specific infusion primers were designed to PCR the heavy chain and light chain from the phagemid DNA. The purified PCR product was infused into human IgG heavy chain and light chain expression vector. The clones were picked for Sanger sequencing to confirm the correct infusion of antibody sequence. Heavy and light chain plasmids were cotransfected in Expi-293 cells, and antibodies were purified by protein A resin.

ELISA of purified NY-ESO-1 antibodies

ELISA was performed similarly as mentioned in phage ELISA, but used purified antibodies in replacement of phage and used HRP anti-human-IgG as a secondary antibody for detection.

Generation of retroviral constructs and transduction

Codon optimized 2D2 scFv was synthesized from Integrated DNA Technologies, Inc (Skokie, Illinois, USA), with a $(G_4S)_3$ linker between the heavy chain and light chain. A GM-CSFR leader sequence was added in front of the viable heavy chain. The fragment was cloned into a pMSGV1 retroviral vector containing CD8α hinge and transmembrane domain, followed by 4-1BB costimulatory domain and CD3ζ signaling domain. All constructs were sequence confirmed.

Blood from healthy donors was obtained from Gulf Coast Regional Blood Center. Fresh PBMCs were isolated with Ficoll reagent following the manufacturer's instructions. Buffy layer was collected and washed twice with PBS. T cell medium suspended PBMCs then were seeded into an antihuman CD3 antibody (OKT3) coated plate for activation. Furthermore, retrovirus was packaged in HEK 293 T cells with envelope plasmid RD114 and packaging plasmid Gag-pol. Virus was harvested at 48-hour and 72-hour post-transfection and filtered with a 0.45 µm filter. Activated PBMCs were transduced twice with retrovirus in the presence of RetroNectin as per the manufacturer's guide. T cells were cultured for 3–7 days before use.

Cytokine detection

HEK293T (HLA-A2$^+$/NY-ESO-1$^-$), MDA-MB-231 (HLA-A2$^+$/NY-ESO-1$^-$ breast cancer cell), MDA-MB-231-A2-ESO (MM231-ESO: HLA-A2$^+$/NY-ESO-1+) and PC3-A2-ESO (NY-ESO-1$^+$/HLA-A2$^+$ prostate cancer cell) were seeded in a 96-well round-bottom plate with triplicates (10^4 cells/well). T cells (0.1 million/well) were cocultured with tumor cells overnight. NY-ESO-1$_{157-165}$ peptide (20 µg/mL) was added into HEK293T cells as a positive control. On the following day, 50 µL supernatants were added into human IFN-γ (1:1000, Thermo Fisher, M700A) precoated and 1% BSA blocked plate for a 1-hour incubation at room temperature with gentle shake. The plate was then washed twice and incubated with a biotin-conjugated IFN-γ antibody (1:1000, Thermo Fisher, M700B) for 1 hour, followed by another two washes and avidin-HRP (1:5000) incubation for 30 min in the dark. After washing, 100 µL TMB was added for reaction, which was stopped

by 50 µL 2.5 N sulfuric acid after 15 min. The absorbance was read on a spectrophotometer (Bio-Tek) at 450 nm.

Flow cytometry

Flow cytometric analysis was performed by using BD LSR II. T cells were stained with protein L and biotinylated HLA-A2/NY-ESO-1 monomer for CD19 CAR-T and 2D2 CAR-T cells, respectively, followed by phycoerythrin (PE)-conjugated streptavidin, while using biotinylated HLA-A2/CMV monomer as control. Tumor cells were stained with mAb 2D2 for 30 min and followed by goat-anti-human IgG-Alexa fluor 594. Data were analyzed with FlowJo V.10.0.7 software (TreeStar).

Confocal imaging

Cells were seeded in a four-chamber glass bottom dish. HEK 293 T cells were pulsed with 20 µg/mL NY-ESO-1 or control peptide. Cells were fixed by 4% PFA for 15 min at room temperature. After washing, cells were blocked with 5% normal goat serum for 1 hour and incubated with 10 µg/mL mAb 2D2 and APC conjugated antihuman HLA-A2 antibody at 4°C overnight. The next day, cells were washed three times with PBS and incubated with 5 µg/mL Alexa Fluor 488 or 594 conjugated goat-anti-human (H+L) secondary antibody for 1 hour in the dark. Nucleus was stained with DAPI for 5 min. Imaging was acquired with a Nikon A1 confocal microscopy.

Immunohistochemistry

Formalin-fixed samples were embedded by paraffin. Blocks were cut at 5 µm and mounted onto positively charged glass slides. After deparaffinization and hydration using graded concentrations of ethanol to deionized water, sections were stained with mouse-anti-human CD3 (Invitrogen, MA5-12577, 1:20) and mouse-anti-human CD8α (Abcam, ab187279, 1:200), respectively. DAB (3,3′diaminobenzidine) was used as a chromogen, followed by nuclear counterstaining. Then slides were washed and dehydrated and covered by coverslips with a permount mounting medium (Fisher, SP15-100). Imaging was captured by Olympus microscopy equipped with a DP74 camera.

LDH cytotoxicity release assay

Transduced T cells were cocultured with tumor cells with a series of effector to target (E:T) ratios in 96-well plates for 6 hours and 24 hours, respectively. Supernatant containing LDH was transferred into a new enzymatic plate for cytotoxicity assay as per the manufacturer's instruction (Promega, G1780). The absorbance was read on a spectrophotometer (Bio-Tek) at 490 nm. Percentage of specific lysis was calculated as the formula: % cytotoxicity = (experimental − effector spontaneous − target spontaneous) / (target maximum − target spontaneous) * 100. All values were substrated by medium control first.

Toxicity studies

HLA-A2 transgenic mice were treated with the same dose used to achieve effective therapy (10 million T cells, intravenously), and the in vivo toxicity was determined by potential clinical signs such as body weight loss and histopathological microscopic evaluation of the major tissues at days 7 and 14.

Statistical analysis

Data were presented as mean±SD or SEM if indicated. Unpaired Student's t-test was used to study the differences between groups; one-way analysis of variance (ANOVA) was used for comparing more than two groups while two-way ANOVA was used for comparing more than two groups at different time points. Kaplan-Meier analysis and log-rank tests were used in the survival comparisons; statistical analysis was performed with GraphPad Prism V.8 (GraphPad Software, Inc). P values of <0.05 were considered to be significant.

RESULTS

Screening and selection of specific scFv for HLA-A2/NY-ESO-1 complex and engineering of full-length human mAb

Human scFv was selected by a negative biopanning of a phage-displayed scFv antibody library on biotinylated HLA-A2/CMV pp65$_{495-503}$ (NLVPMVATV) control peptide monomer followed by a positive biopanning on HLA-A2/NY-ESO-1$_{157-165}$ (SLLMWITQC) monomer. Hence, phages bound to HLA-A2 and an irrelevant peptide or biotin would have been eliminated in this step (figure 1A). After 3~4 rounds of panning, 40 clones were found to have positive binding to HLA-A2/NY-ESO-1$_{157-165}$ via phage ELISA (figure 1B, online supplemental figure S1A). Those clones were sequenced, and diversity of genotype was analyzed according to the IMGT repertoire (www.imgt.org) (online supplemental figure S1B). Ten clones with unique antibody sequences were further cloned into expression vectors. Among them, eight fully human IgG1 antibodies were expressed and purified. Two purified mAb E5 and mAb 2D2 had high specificity in recognition of 10 µg/mL HLA-A2/NY-ESO-1$_{157-165}$ complex but not HLA-A2/CMV pp65$_{495-503}$ complex (online supplemental figure S1C). However, mAb E5 showed no recognition of HLA-A2/NY-ESO-1$_{157-165}$ complex at a low concentration of 1 µg/mL, while mAb 2D2 maintained the specificity in recognizing target antigen but not control antigen (figure 1C). An antibody titration experiment against HLA-A2/NY-ESO-1$_{157-165}$ revealed that EC$_{50}$ of E5 was 66 nM, while mAb 2D2 had an EC$_{50}$ of 0.608 nM (figure 1D, online supplemental figure S1D). This may explain the difference in recognition of HLA-A2/NY-ESO-1$_{157-165}$ between mAb E5 and mAb 2D2 mAb at the low concentration. Thus, mAb 2D2 was selected for further studies.

Characterization of mAb 2D2

To further characterize the specificity of mAb 2D2, we first measured the affinity of mAb 2D2 to HLA-A2/NY-ESO-1$_{157-165}$ complex by the biolayer interferometry on an Octet instrument. A moderate high affinity
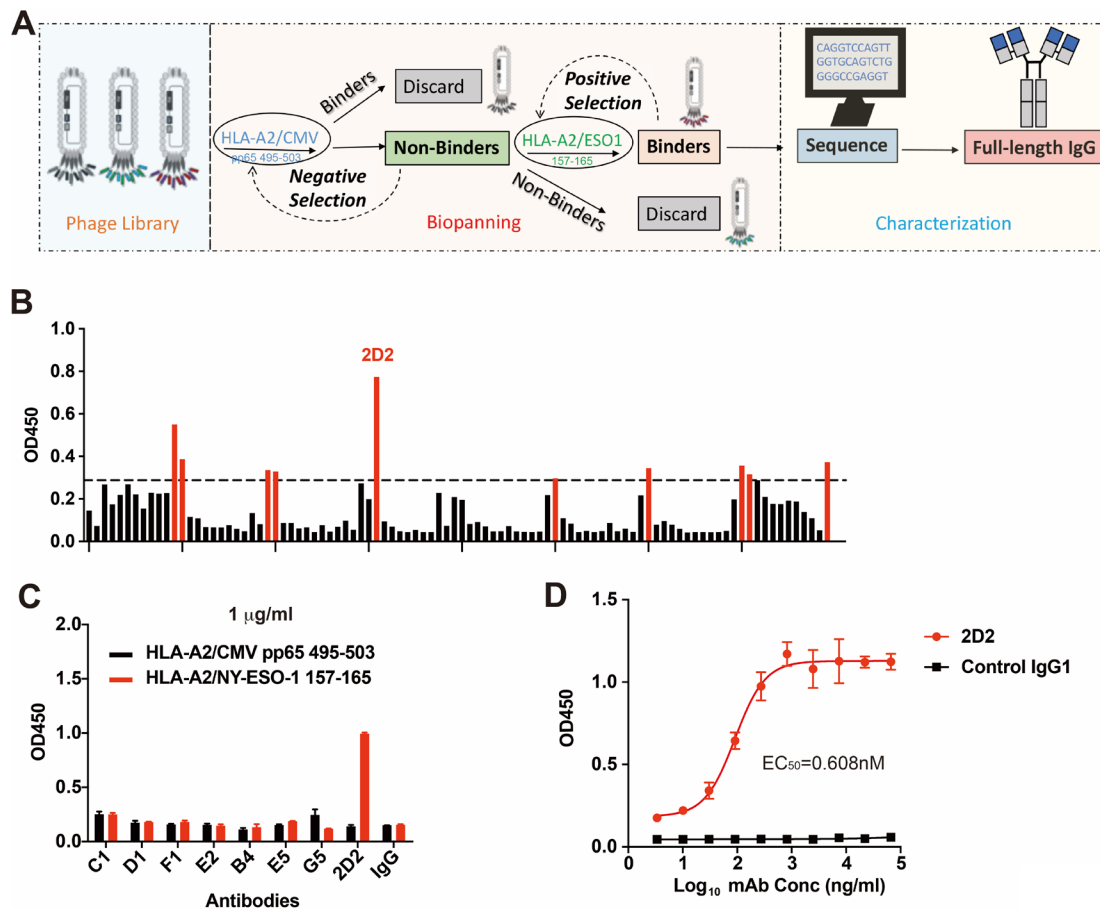
Figure 1 Selection of scFvs specific for HLA-A2/NY-ESO-1 complex. (A) The schematic diagram of screening of HLA-A2/NY-ESO-1$_{157-165}$ complex specific antibodies from human scFv phage-displayed library. Phage library was negative and positive selected against HLA-A2/CMV pp65$_{495-503}$ and HLA-A2/NY-ESO-1$_{157-165}$, respectively. Final binders were sequenced and converted to full-length IgG1. (B) Example plate of phage ELISA against biotin conjugated HLA-A2/NY-ESO-1$_{157-165}$ monomer. Positive clones were considered as three times higher than the threshold calculated by the average value of negative control wells. (C) ELISA validation of purified monoclonal antibodies against HLA-A2/NY-ESO-1$_{157-165}$ and control pMHC complex at concentration of 1 µg/mL. (D) Antibody titration of positive clone mAb 2D2 via ELISA. mAb, monoclonal antibody; scFvs, single-chain variable antibody fragments.

interaction between mAb 2D2 to HLA-A2/NY-ESO-1$_{157-165}$ complex was detected in the Kd value of 5.74±0.221 nM (figure 2A). Flow cytometry showed that mAb 2D2 specifically recognized NY-ESO-1$_{157-165}$ peptide-pulsed HEK 293 T cells, which form HLA-A2/NY-ESO-1$_{157-165}$ complex, in a dose-dependent manner, but not CMV pp65$_{495-503}$ peptide-pulsed HEK 293 T cells that present HLA-A2/CMV pp65$_{495-503}$ control complex (figure 2B). Increasing concentrations of mAb 2D2 from 0.5 µg/mL to 4 µg/mL dramatically enhanced the percentage of positive cells from 32.7% to 80.2%, while further increasing the concentration of antibody only slightly changed the positive rate (figure 2B). Similarly, analysis of mean fluorescence intensity also indicated the specificity of mAb 2D2 binding to HLA-A2/NY-ESO-1$_{157-165}$ complex, with a saturated concentration above 16 µg/mL (figure 2C). We also used immunofluorescence to confirm our result by confocal microscopy imaging. HEK 293 T cells were pulsed with NY-ESO-1$_{157-165}$ and CMV pp65$_{495-503}$ peptide, respectively. Cells were costained with anti-HLA-A2 and mAb 2D2, as well as DAPI for the nucleus. mAb 2D2

colocalized with HLA-A2 in NY-ESO-1$_{157-165}$ peptide-pulsed HEK 293 T cells but not in CMVpp65$_{495-503}$ control peptide-pulsed cells (figure 2D), indicating the antigen-specific binding of mAb 2D2 on the cell surface, which is a critical prerequisite for targeted therapy such as CAR-T.

Retrovirally transduced T cells express the 2D2-CAR

The 2D2-CAR was engineered using variable heavy and light chain sequences from the 2D2 scFv connected by a (Gly4Ser)3 flexible linker. The 2D2 scFv with a GM-CSFR leader sequence was ligated upstream to the CD8α hinge and transmembrane and 4-1BB costimulatory domain and CD3ζ signaling domain. The resulting 2D2-BBZ gene was cloned into a pMSGV1 gamma-retroviral vector and confirmed by sequencing (figure 3A). Following retroviral transduction, T cells expressed high levels of 2D2-CAR, as assessed by flow cytometric analysis using a biotinylated HLA-A2/NY-ESO-1$_{157-165}$ monomer followed by streptavidin-PE (figure 3B). The transduction efficiency of the CAR T cells was between 30% and 90% for all experiments. To confirm that the 2D2-CAR was not artificially binding to
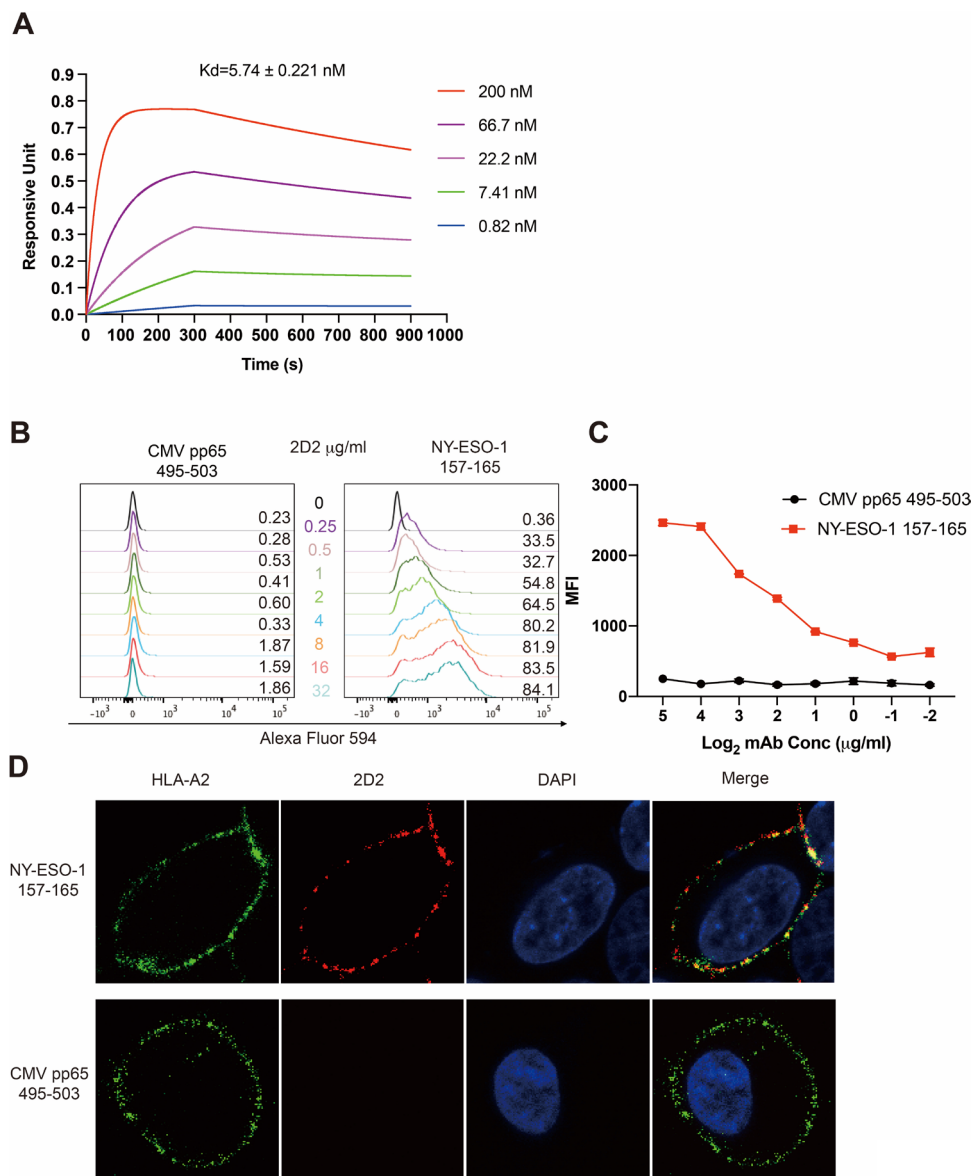
Figure 2 Characterization of mAb 2D2 and its specificity. (A) Binding affinity of mAb 2D2 to the HLA-A2/NY-ESO-1$_{157-165}$ complex measured by the biolayer interferometry (BLI) on an Octet instrument. (B) Flow cytometry analysis of mAb 2D2 with a series of dilution. HEK 293T cells were pulsed with 20 µg/mL NY-ESO-1$_{157-165}$ or CMV pp65$_{495-503}$ peptide for 1 hour at 37°C. Cells were washed and stained with a series dilution of mAb 2D2 followed by Alexa Fluor 594 conjugated goat-anti-human (H+L) secondary antibody. mAb 2D2 could recognize NY-ESO-1$_{157-165}$ pulsed HEK 293T cells but not CMV pp65$_{495-503}$ peptide-pulsed HEK 293T cells. (C) Mean fluorescence intensity analysis from panel B. (D) Confocal imaging of mAb 2D2 staining in NY-ESO-1$_{157-165}$ peptide-pulsed HEK 293T. HEK 293T cells were pulsed with 20 µg/mL NY-ESO-1$_{157-165}$ or CMV pp65$_{495-503}$ peptide for 1 hour. Cells were fixed with 2% PFA and then stained with APC conjugated HLA-A2 and mAb 2D2 followed by Alexa Fluor 594. DAPI was used for nuclear staining. mAb, monoclonal antibody.

HLA-A2/NY-ESO-1$_{157-165}$ monomer due to high avidity for the antigen, cytomegalovirus (CMV) pp65$_{495-503}$-HLA-A2 monomer was used to stain CAR T cells. No binding of the HLA-A2/CMVpp65$_{495-503}$ monomer was observed on 2D2-CAR T cells (online supplemental figure S2A).

2D2-CAR T cells specifically recognize and lyse HLA-A2+, NY-ESO-1+ cells

The specific recognition of 2D2-CAR T cells was assessed by IFN-γ ELISA against a range of HLA-A2+ and/or NY-ESO-1+ cancer cell lines and HLA-A2+ cells pulsed with NY-ESO-1$_{157-165}$ peptide. 2D2-CAR T cells specifically

recognized TAP-deficient T2 cells (HLA-A2+) pulsed with NY-ESO-1$_{157-165}$ peptide, but not T2 cells loaded with CMV pp65$_{495-503}$ peptide (figure 3C). To further determine the specificity of 2D2-CAR-T cells against NY-ESO-1 petide, alanine scaning within NY-ESO-1 peptide was conducted. Nine peptides containing an alanine substitution at each position, together with wildtype NY-ESO-1 peptide and control peptide derived from a different cancer testis antigen, were pulsed onto T2 cells at a concentration of 2 µg/mL. 2D2-CAR-T cells were cocultured with T2 cells pulsed with different peptides to determine specific
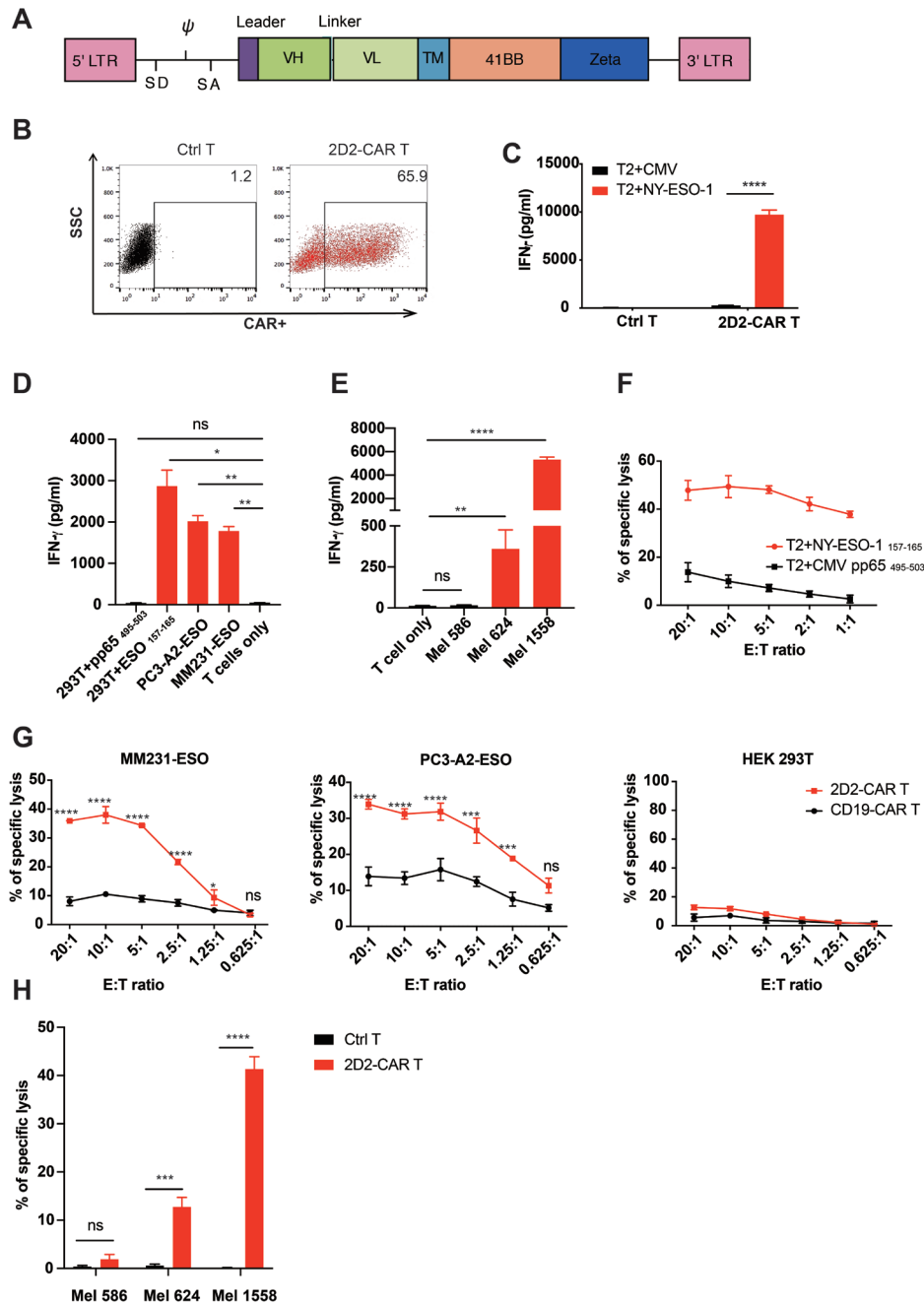
Figure 3 2D2-CAR T cells specifically recognize and lyze HLA-A2+/NY-ESO-1+cells in vitro. (A) Schematic diagram of 2D2 CAR construct. 2D2 scFv was cloned into a pMSGV1 retroviral vector with CD8α hinge and transmembrane, 4-1BB co-stimulatory, and CD3ζ signaling domain. (B) Surface expression of CAR detected by HLA-A2/NY-ESO-1$_{157-165}$ complex. (C) IFN-γ cytokine release measured by ELISA. T2 cells (HLA-A2+) were pulsed with 20 µg/mL NY-ESO-1$_{157-165}$ or CMV pp65$_{495-503}$ peptide for 1 hour at 37°C. 2D2-CAR T cells were cocultured with target cells with a 10:1 (E: T) ratio overnight. (D) IFN-γ cytokine release measured by ELISA. 2D2-CAR T cells were cocultured with HEK 293 T cells (HLA-A2+) pulsed with NY-ESO-1$_{157-165}$ or CMV pp65$_{495-503}$ peptide, PC3-A2-NY-ESO-1, MDA-MB-231-NY-ESO-1(HLA-A2+) at 10:1 ratio overnight. (E) 2D2-CAR T cells were cocultured with endogenously expression cell lines Mel 586 (A2-/NY-ESO-1+), Mel 624 (A2+/NY-ESO-1+), and Mel 1558 (A2+/NY-ESO-1+) at a 20:1 ratio overnight. (F) LDH cytotoxicity assay. 2D2-CAR T cells were cocultured with T2 cells that were pulsed with 20 µg/mL NY-ESO-1 or CMV peptide for 1 hour for 4 hours. (G) LDH cytotoxicity assay. 2D2-CAR T cells were cocultured with MDA-MB-231-NY-ESO-1 and PC3-A2-NY-ESO-1 and HEK293T for 24 hours, respectively. (H) LDH cytotoxicity assay for 2D2-BBZ and control T cells against Mel 586, Mel 624, and Mel 1558. *P<0.05; **p<0.01; ***p<0.001; ****p<0.0001. CAR, chimeric antigen receptor; ns, not significant.

recognition. We found that alanine substitution of the residue positions 4 (Met) and 5 (Trp) completely abolished T cell activity. Furthermore, substitution of residue positions 2 (Leu) and 3 (Leu) also markedly reduced T cell activity, while substitution of residue position 1 (Ser) reduced T cell activity but statistically not significant

(online supplemental figure S2B). These results suggest that residue positions 2, 3, 4 and 5 are critically important for 2D2-CAR-T cell recognition and specificity of NY-ESO-1 peptide, while the C-terminus of the NY-ESO-1 peptide may not contribute to the interaction with 2D2-CAR-T cells. Next, we showed that 2D2-CAR T cells could recognize a range of tumor types including HEK 293T (HLA-A2+) pulsed with NY-ESO-1$_{157-165}$ peptide, triple-negative breast cancer overexpressing NY-ESO-1 (MDA-MB-231-ESO1) (HLA-A2+), and prostate cancer cells expressing HLA-A2 and NY-ESO-1 (PC3-A2-ESO1), as well as Mel 624 and Mel 1558 (endogenously expressing HLA-A2 and NY-ESO-1 double-positive tumor cell lines) but not Mel586 (HLA-A2-, NY-ESO-1+) (figure 3D,E). Proliferation assay using CFSE labeled T cells indicated 2D2-CAR specific T cells divided quickly after coculture with tumor cells (online supplemental figure S2C). Activation markers such as CD25 and CD69 were significantly up-regulated in both CD4 and CD8 T cells on recognition of tumor cells (Fig. S2D, E). To demonstrate the killing ability of 2D2-CAR T cells, a range of effector-to-target ratios were set. 2D2-CAR T cells could lyze T2 cells pulsed with NY-ESO-1$_{157-165}$ but not CMV pp65$_{495-503}$ peptide (figure 3F). Furthermore, 2D2-CAR T cells exhibited specific killing of MDA-MB-231-NY-ESO1 and PC3-A2-NY-ESO1 tumor cell lines as compared with control T cells or genetically engineered T cells targeting CD19 (19BBZ) (figure 3G). However, there was no difference between 2D2-CAR and CD19-CAR against a control cell line HEK 293T (figure 3G). Significantly, 2D2-CAR-T could also kill Mel 624 and Mel 1558 but not Mel 586 (figure 3H). Moreover, a similar experiment was conducted by coculturing 2D2-CAR T cells with CFSE labeled, NY-ESO-1$_{157-165}$ peptide-pulsed T2 cells overnight. Flow cytometry analyzed the remaining CFSE positive tumor cells. 2D2-CAR T cells dramatically eliminated tumor cells compared with control CD19 CAR-T cells (0.28% vs 28.1%) (online supplemental figure S2F). More importantly, NY-ESO-1 mRNA expression level can be significantly induced by FDA-approved DNA demethylating agent 5-aza-2′-deoxycytidine (DAC) in MCF7 and MDA-MB-231 tumor cell lines (online supplemental figure S3A). Enhanced NY-ESO-1 expression led to tumor recognition by 2D2-CAR-T cells and T cell-mediated killing ability (online supplemental figure S3B,C).

2D2-CAR T cells prolong the survival of mice bearing triple-negative breast cancer in vivo

To assess the efficacy of 2D2-directed CAR T cells in a solid tumor model in vivo, human triple-negative breast cancer MDA-MB-231 expressing NY-ESO-1 was injected into the fat pad of NSG mice. Mice were randomized to be treated with 2D2-CAR T cells or control T cells via intravenous 4 days after tumor inoculation (figure 4A). A significant release of IFN-γ in mice serum was detected on day 5 post adoptive cell transfer (figure 4B). A single dose of 2D2-CAR T cells significantly impaired tumor growth compared with mice from the control group (figure 4C). Mice were sacrificed, and tumors were harvested on day

30. 2D2-CAR T cells treated mice had smaller tumor volume (figure 4D), and the weight of tumor was significantly reduced about 50% compared with control mice (p=0.0018) (figure 4E). In addition, mice treated with 2D2-CAR T cells greatly enhanced overall survival with a median survival of 41 days (Ctrl vs 2D2-CAR T: p=0.0027) (figure 4F). Through further investigation in the mice spleen, we detected more CD3 +T cells in 2D2-CAR-T cell treated group than the control group (online supplemental figure S4A). The CD3 positive T cells were counted, and the percentage in the spleen indicated 10-fold higher in the 2D2-CAR-T group compared with the control group (online supplemental figure S4B). Furthermore, significantly T cell infiltration (CD3 and CD8) into tumor cells was detected in the tumor section from 2D2-CAR T cell treated mice (online supplemental figure S4C,D). These data suggest that 2D2-CAR T cells can effectively infiltrate into the tumor, kill tumor cells, impair tumor growth and prolong mice overall survival.

2D2-CAR T cells show antitumor activity against an endogenously expressing HLA-A2/NY-ESO-1 tumor model in vivo

To further demonstrate the antitumor response in a more clinically relevant application, we chose a tumor cell line Mel1558 that endogenously expresses HLA-A2/NY-ESO-1. Two million tumor cells were subcutaneously implanted at right flank of NSG mice. total of 2.5 million 2D2-CAR T cells were injected on day 4 followed by 50,000 IU rhIL-2 intraperitoneally. Cytokine was detected on day 6 after T cell injection from mice serum (figure 5A). We noticed a significant difference in IFN-γ release between control and treated groups, even though the amount is very low (figure 5A). 2D2-CAR T-cell treated mice had a significant reduction in tumor growth starting from day 35 (figure 5B). The tumors harvested from 2D2-CAR T cell treated mice were about 50% smaller compared with control groups (figure 5C). Further analysis in the tumor section by IHC revealed that a significant increment of T cells infiltrated in the tumor in the 2D2-CAR T treated group than the control group (figure 5D). Consistently, flow cytometry also proved the existence of T cells in the tumor section with more than fivefold higher in the 2D2-CAR-T group (figure 5E). All these data suggest that 2D2-CAR T cells can inhibit the growth of tumor endogenously expressing A2/NY-ESO-1 in vivo.

2D2-CAR T cells show no evidence of potential toxicity in vivo

To evaluate the potential side effects of 2D2-CAR T cells, human HLA-A2 transgenic NSG (NSG-A2) mice (n=6) were treated with 1×10^{7} of 2D2-CAR T cells in 200 μL PBS or an equivalent volume of PBS as control. Body weight and health condition were monitored daily. Mice were euthanized to harvest key tissue organs on day 7 and day 14 for pathological analysis (figure 6A). We found that 2D2-CAR-T cell treatment did not cause any marked decrease in mouse body weight and displayed no significant difference in growth compared with control group
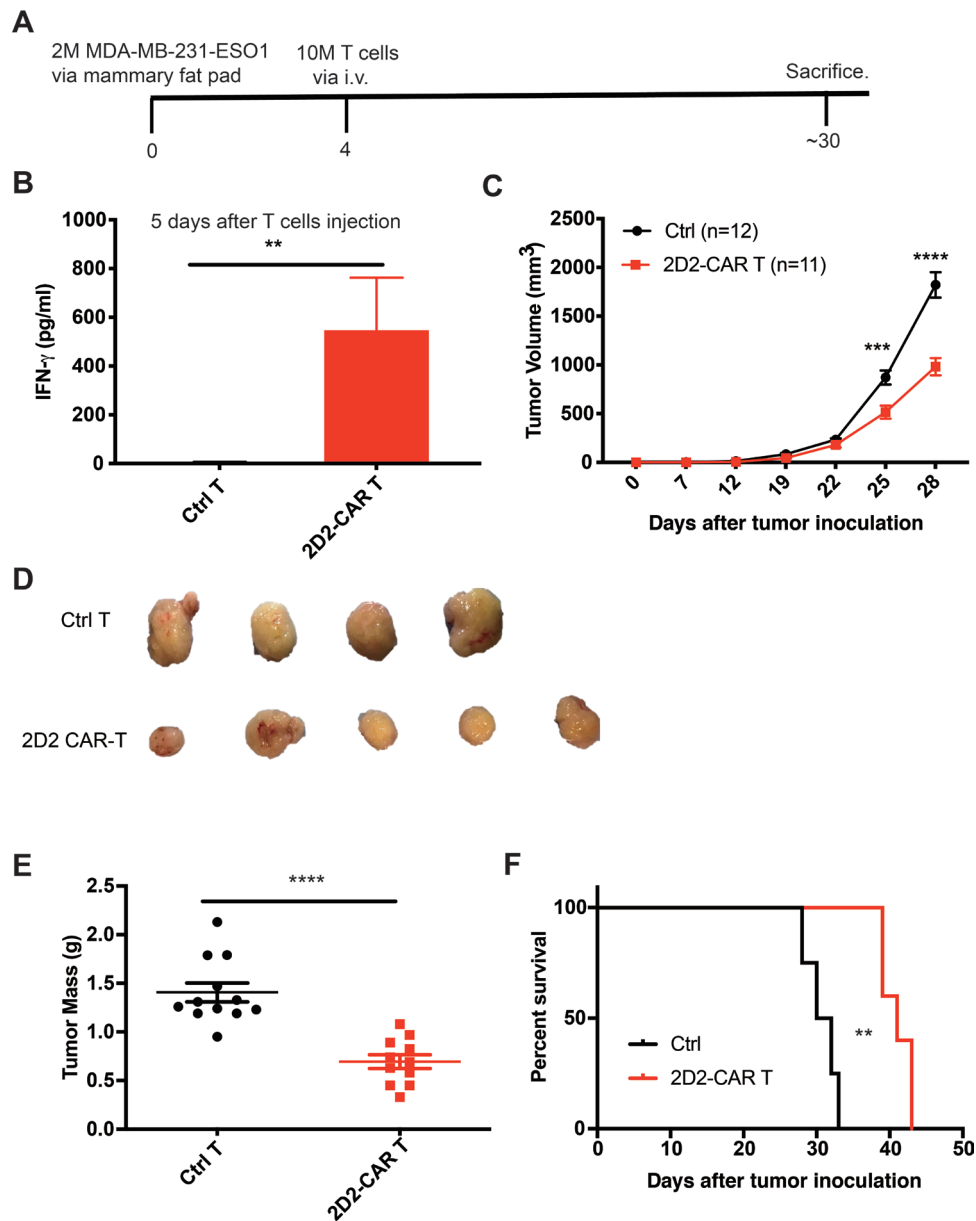
Figure 4 2D2-CAR T cells impair tumor growth and prolong the survival of mice bearing triple-negative breast cancer in vivo. (A) A schematic diagram of the animal experiment. Female NSG mice were injected with 2 million MDA-MB-231 expressing NY-ESO-1 at the fat pad on day 0. On day 4, mice were randomly separated in to control group (n=4) and treatment group (n=5). Ten million 2D2-CAR-T cells or control T cells suspended in 200 µL PBS were injected intravenously followed by three continuous injections of 50,000 units of rhIL-2 intraperitoneally. (B) Representative IFN-γ ELISA with mice serum at day 5 after T cells injected. (C) Tumor growth combined from three independent experiments between the control group (n=12) and 2D2-CAR T cells treated group (n=11) was analyzed. Tumor volume was calculated by ½ (L*W∧2). (D) Representative picture of tumor at the time of endpoint. (E) Tumor weight from three independent experiments was quantified. (F) Representative survival analysis of MBA-MD-231-NY-ESO-1 bearing mice treated with 2D2-CAR T cells compared with the control group. Mice were sacrificed when the tumor reaches 2 cm in diameter, which was considered as an endpoint. Data in figure part B were present as mean (SD). Difference between the control group and treatment group was analyzed by unpaired Students' t-test. Data in figure parts C and E were presented as mean (SE). Difference was analyzed by two-way ANOVA followed by multiple comparisons with Bonferroni adjustment. Data in figure part F was analyzed by Kaplan-Meier survival analysis with a log-rank test. **P<0.01; ***p<0.001. ANOVA, analysis of variance; CAR, chimeric antigen receptor.

(figure 6B). Major organs including brain, heart, liver, spleen, lung, and kidney were freshly collected from euthanized mice on days 7 and 14 after 2D2-CAR-T cell treatment. There was no siginificant difference in organ weight between 2D2-CAR-T cell-treated group and control group (online supplemental table S1). Consistently, we did not observe any potential tissue damage, such as organ discoloration, apparent side/shape change, or liquid in the abdominal/thoracic cavity. H&E staining and microscopic examination did not show obvious abnormality
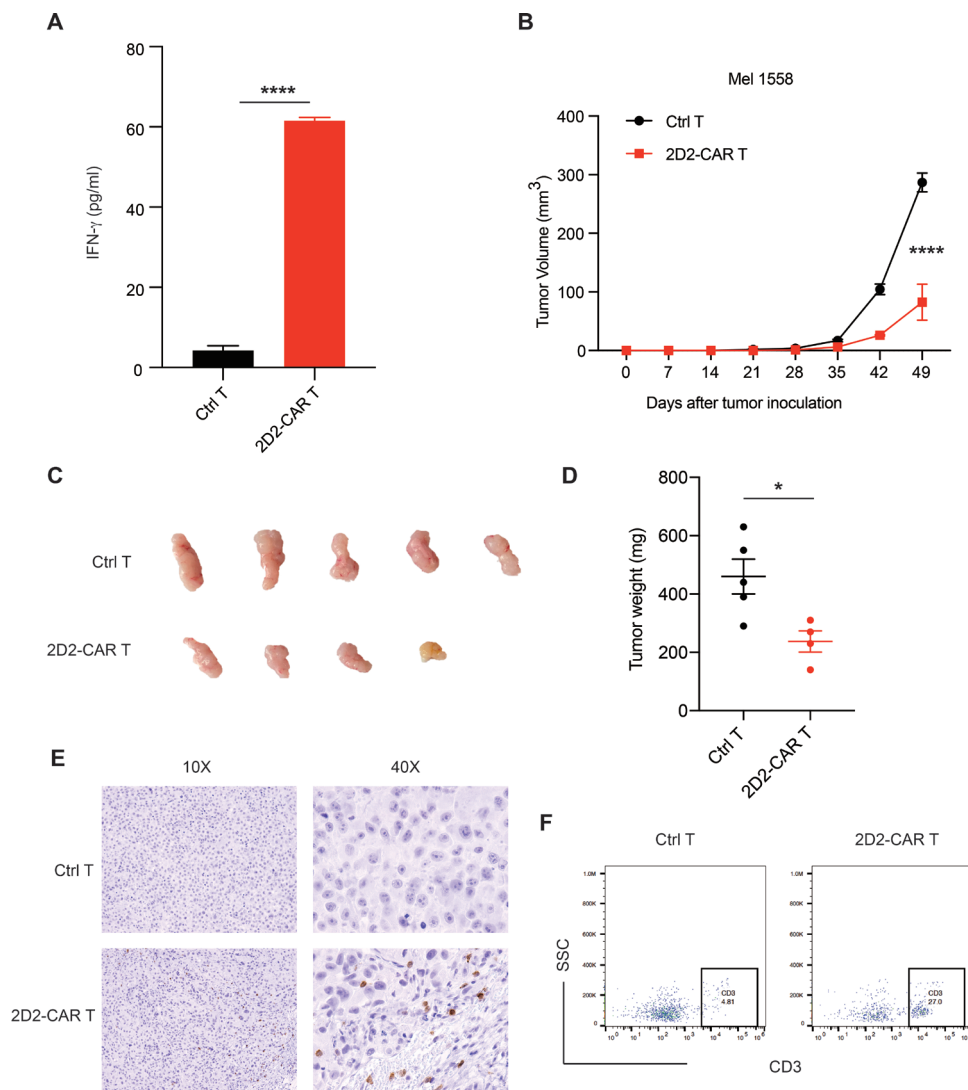
Figure 5 2D2-CAR T cells demonstrate antitumor activity against an endogenously expressing A2/ESO melanoma tumor model in vivo. (A) 2 million Mel 1558 tumor cells were inoculated at the right flank of NSG mice followed by control T (n=5) or 2D2-CAR T cells (n=4) treatment, respectively. IFN-γ was detected from the mice serum harvested 6 days after T cell injection. (B) Tumor growth of Mel 1558 in NSG mice was measured weekly via calipers. 2D2-CAR T cells treated mice had significantly impaired tumor growth. (C) Image of tumor size harvested from mice. (D) Tumor weight of the tumor. (E) T cells infiltration into the tumor were detected by CD3 IHC. (F) T cells infiltration into the tumor were detected by flow cytometry. *P<0.05; ****p<0.0001. CAR, chimeric antigen receptor.

or pathology in the brain, heart, liver, spleen, lung, or kidney from 2D2-CAR-T cell injected mice compared with the control group (figure 6C). Furthermore, we performed CBC and biochemistry analysis (Superchem) of mice treated with 2D2-CAR-T cells and found a slight but not significantly increase in absolute blood cell numbers such as white cell count, red blood cells, neutrophils, monocytes, eosinophils, and basophils, in 2D2-CAR-T cell treated mice compared with PBS treated mice. The relative number was slightly reduced in neutrophils and significantly increased in monocytes. No appreciable changes in platelet, hemoglobin, hematocrit, mean corpuscular volume, mean corpuscular hemoglobin, and mean corpuscular hemoglobin concentration were observed (online supplemental table S2). In the serum chemistry study, we did not observe any significant

difference between 2D2-CAR-T cells treated mice and PBS treated control mice. Liver function was evaluated by the serum level of total protein, albumin, globulin, albumin/globulin ratio, aspartate transaminase, alanine transaminase, Alkaline phosphatase, gamma-glutamyl transferase, and total bilirubin. Key electrolytes such as phosphorus, chloride, calcium, magnesium, sodium, potassium, and sodium/potassium ratio were balanced in both groups. Concentrations of glucose, cholesterol, and triglyceride were in the normal range. Kidney function as measured by blood urea nitrogen (BUN), creatinine and BUN/creatinine ratio, pancreatic function as measured by amylase and precision PSL, and muscle function measured by creatine phosphokinase, were all normal in 2D2-CAR-T treated mice compared with PBS treated mice (online supplemental figure S5). These results
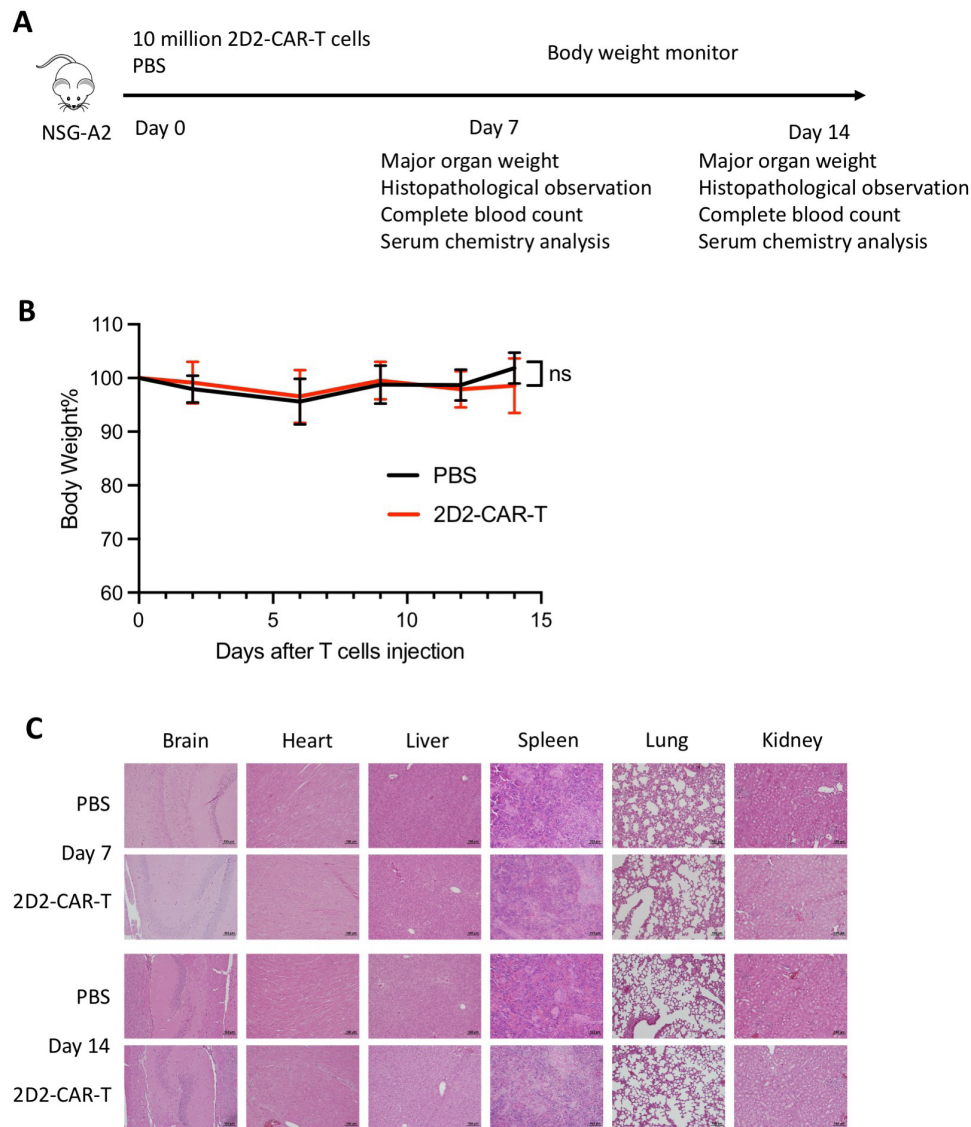
Figure 6 Safety assessment of 2D2-CAR T cells in vivo. (A) A schematic diagram of the animal experiment. NSG-A2 mice were infused with 1×10^7 2D2 CAR T cells or PBS on day 0. Body weight was measured as indicated. On day 7 and day 14, mice were sacrificed for histopathology and hematology assessment. (B) Body weight change after T cells injection. (C) H&E staining for the key organs, heart, spleen, lung, kidney, brain, and liver with 10× magnification. CAR, chimeric antigen receptor; ns, not significant.

suggest that 2D2-CAR-T cell treatment does not induce any potential toxicity or tissue damage in NSG-A2 mice.

DISCUSSION

In this study, we identified mAb 2D2 as a novel TCR-like human full-length IgG1 monoclonal antibody against an intracellular cancer-testis antigen NY-ESO-1 presented by HLA-A2 molecules. The mAb 2D2 could specifically recognize HLA-A2/NY-ESO-1$_{157\text{-}165}$ monomer, NY-ESO-1$_{157\text{-}165}$ pulsed T2 or HEK 293T cells, and tumor cells expressing HLA-A2 and NY-ESO-1, but not HLA-A2/CMV pp65$_{495\text{-}503}$. We further show that genetically engineered 2D2-CAR T cells could specifically recognize HLA-A2/NY-ESO-1 complex and lyse tumor cells both in vitro and in vivo. Mice treated with 2D2-CAR T cells significantly

impaired the growth of A2 and NY-ESO-1 double positive breast cancer cells and enhanced overall survival. Notably, no adverse effect was observed in the key organs of the normal mice treated with 2D2-CAR T cells along, demonstrating the safety of the 2D2-CAR T cells.

A previous study used a semisynthetic Fab repertoire to identify antibodies that could bind to HLA-A2/NY-E-SO$_{157\text{-}165}$.[35] Although they removed streptavidin binders, there was no negative selection round against the HLA-A2 complex with non-relevant peptides. The affinity of antibody (3M4E5) isolated from the screening was 60 nM, which was further modified to increase the affinity via the comparison between the high-resolution structure of 1G4 TCR and 3M4E5 bound to HLA-A2/NY-ESO-1$_{157\text{-}165}$. Using computer model analysis, a new library with point

mutations in the residues not contacting with the peptide was generated.[36] This super-high affinity antibody (T1) exceeded the affinity of TCR by 1000-fold. Specific lysis of HLA-A2 positive T2 cells pulsed with NY-ESO-1 peptide was observed. However, no killing activity of primary tumor cells was demonstrated. In a subsequent study using a CAR construct containing an scFv from T1 antibody, it was found that T1 scFv-CAR-T cells failed to show the antigen specificity probably due to the high affinity of T1 antibody to HLA-A2/NY-ESO-1$_{157-165}$ complex as well as HLA-A2 molecules.[37] Similar to TCR,[38–41] these studies suggest that increasing TCR-like antibody affinity may increase the likelihood of cross-reactivity against HLA molecules. Therefore, mAb 2D2 has an affinity of 5.74 nM, a moderate high affinity for a monoclonal antibody, which somehow maintains the specificity, promoting the success of CAR-T therapy. Interestingly, the immunoglobin type of the mAb 2D2 VL chain was the same as T1, while it differed in the heavy chain variable region. However, 2D2-CAR T cells did not display 'off-target' issues, as demonstrated by our in vivo experiments.

Even though antibodies usually have higher affinity than TCRs, CAR-T cells derived from TCR-like antibodies may need a higher density of pMHC complex presented at the cell surface to achieve a similar level of activation compared with TCR-T cells.[42] αβ-TCR-T cells with relatively low-affinity maintain the specificity and cytotoxic activity, while the high-affinity CAR-T cells may reduce specificity and killing ability.[43] One possible reason is the difference of conformation between in vitro refolded complex and bona fide pMHC complex on the cell surface for TCR-like antibody recognition. To compare HLA-A2 NY-ESO-1 specific (A2-ESO TCR)-T cells with 2D2-CAR-T cells, we cloned 1G4 with two amino acid substitutions[44] into retroviral expression vector. The same numbers of A2-ESO TCR T- and 2D2 -CAR-T cells were cocultured with CMV pp65$_{495-503}$ peptide or NY-ESO-1$_{157-165}$ peptide, respectively. We found that A2-ESO TCR-T cells released higher (10-fold) IFN-γ than 2D2-CAR-T cells in response to A2/NY-ESO-1 complex (online supplemental figure S6A). Importantly, the killing activity of 2D2-CAR-T cells was similar to that of A2-ESO TCR-T cells (online supplemental figure S6B). A previous study shows that the target antigen density required for inducing T cell cytokine production is much higher than that required for stimulating CAR-mediated lysis.[45] The lowest density for CD20-specific CAR-T cells to lyse target cells is ~200 molecules per cell, but cytokine production required a higher density of CD20 (~5000 molecules per cell).[45] Generally, TCR-T cells require 10 pMHC complexes per cell on the target surface to be activated, while CAR-T cells require more than 100 copies per cell.[46] Importantly, the lower cytokine production by 2D2 CAR-T cells may reduce the risk of potential toxicity associated with the cytokine storm, while maintaining similar killing ability of tumor cells. To further test this possibility, we performed in vivo experiment to demonstrate the therapeutic efficacy of A2-ESO TCR-T cells and 2D2-CAR-T cells. We found that both A2-ESO TCR-T cells and 2D2-CAR-T cells showed strong antitumor response (online supplemental figure S6C). Finally, A2-ESO TCR α and β chains may mispair with endogenous TCR α and β chains, causing potential off-target cross reactivity, while 2D2-CAR-T cells could not mispair with endogenous TCR α and β chains. Thus, the lower amounts of cytokine release and no potential mispairing of 2D2 CAR-T cells may have advantages over A2-ESO TCR-T cells. However, further studies are needed to investigate potential clinical application.

Currently, CAR-T cell technology does not work well in the solid cancers. 2D2-CAR T cells could not completely eradicate tumor cells in mouse models. We showed that the in vitro cytolytic activity of 2D2-CAR-T cells was correlated with the level of HLA-A2/NY-ESO-1 complex on the cell surface, suggesting that the low cytolytic activity of 2D2-CAR-T cells toward MDA-MB-231-ESO and Mel1558 in vivo is due to a low density of HLA-A2/ NY-ESO-1 complex on the cell surface. Furthermore, T cell trafficking and persistence could also influence the anti-tumor activity of CAR-T or TCR-T cells in vivo. We noticed that T cells would die within a week after injection into the NSG mice in the absence of antigen stimulation or IL-2 (data not shown). Murine CAR-T cells may exert superior antitumor activity in immunocompetent mice.[47] Combination therapy together with checkpoint blockade or negative regulator inhibition may also augment antitumor activity in vivo.[48] T cell trafficking to tumor sites is critically important for CAR-T cell therapy in the solid cancers. For example, CXCR3 and CCR5 are often highly expressed in tumor-infiltrating lymphocytes from melanoma, colorectal and breast cancers, implying the importance in regulating T cell trafficking.[49] Thus, further studies are needed to promote 2D2-CAR-T cell trafficking and persistence in the solid cancer and overcome immune suppression in the tumor microenvironment, thus developing more effective CAR-T or TCR-like CAR-T cell therapy.

In summary, our results presented here provide a proof of concept that TCR-like antibody derived CAR-T cells could successfully inhibit tumor cell growth and enhance mouse overall survival. Unlike current CAR technology that only recognizes surface antigens, TCR-like CAR may broaden the scope of target antigens, including intracellular antigens. The specificity and cytotoxicity of our TCR-like CAR would significantly impact our ability to develop new immunotherapy against various types of cancer.

Author affiliations
[1]Keck School of Medicine, University of Southern California, Los Angeles, California, USA
[2]Center for Inflammation and Epigenetics, Houston Methodist Research Institute, Houston, Texas, USA
[3]Institute of Biosciences and Technology, College of Medicine, Texas A&M University, Houston, Texas, USA
[4]Texas Therapeutics Institute, Brown Foundation Institute of Molecular Medicine, University of Texas Health Science Center at Houston, Houston, Texas, USA
[5]Xiangya School of Medicine, Xiangya Hospital, Central South University, Changsha, Hunan, People's Republic of China

[6]Neurosurgical Oncology in the Department of Neurosurgery, Cedars-Sinai Medical Center, Los Angeles, California, USA

ORCID iDs
Wei Xiong http://orcid.org/0000-0002-8087-5047
Rongfu Wang http://orcid.org/0000-0002-8834-2763

REFERENCES

1. Weiner LM, Dhodapkar MV, Ferrone S. Monoclonal antibodies for cancer immunotherapy. *Lancet* 2009;373:1033–40.
2. Grupp SA, Kalos M, Barrett D, *et al*. Chimeric antigen receptor-modified T cells for acute lymphoid leukemia. *N Engl J Med* 2013;368:1509–18.
3. Porter DL, Levine BL, Kalos M, *et al*. Chimeric antigen receptor-modified T cells in chronic lymphoid leukemia. *N Engl J Med* 2011;365:725–33.
4. Ma S, Li X, Wang X, *et al*. Current progress in CAR-T cell therapy for solid tumors. *Int J Biol Sci* 2019;15:2548–60.
5. Sterner RC, Sterner RM. CAR-T cell therapy: current limitations and potential strategies. *Blood Cancer J* 2021;11:69.
6. Martinez M, Moon EK. CAR T cells for solid tumors: new strategies for finding, infiltrating, and surviving in the tumor microenvironment. *Front Immunol* 2019;10:128.
7. Xu Y, Salazar Georgina To'a, Zhang N, *et al*. T-cell receptor mimic (TCRm) antibody therapeutics against intracellular proteins. *Antib Ther* 2019;2:22–32.
8. Wang R-F, Wang HY. Immune targets and neoantigens for cancer immunotherapy and precision medicine. *Cell Res* 2017;27:11–37.
9. Han J, Chu J, Keung Chan W, *et al*. CAR-Engineered NK cells targeting wild-type EGFR and EGFRvIII enhance killing of glioblastoma and patient-derived glioblastoma stem cells. *Sci Rep* 2015;5:11483.
10. Odunsi K, Jungbluth AA, Stockert E, *et al*. NY-ESO-1 and LAGE-1 cancer-testis antigens are potential targets for immunotherapy in epithelial ovarian cancer. *Cancer Res* 2003;63:6076–83.
11. Jungbluth AA, Chen YT, Stockert E, *et al*. Immunohistochemical analysis of NY-ESO-1 antigen expression in normal and malignant human tissues. *Int J Cancer* 2001;92:856–60.
12. Wang RF, Wang X, Atwood AC, *et al*. Cloning genes encoding MHC class II-restricted antigens: mutated CDC27 as a tumor antigen. *Science* 1999;284:1351–4.
13. Chen YT, Scanlan MJ, Sahin U, *et al*. A testicular antigen aberrantly expressed in human cancers detected by autologous antibody screening. *Proc Natl Acad Sci U S A* 1997;94:1914–8.
14. Wang RF, Johnston SL, Zeng G, *et al*. A breast and melanoma-shared tumor antigen: T cell responses to antigenic peptides translated from different open reading frames. *J Immunol* 1998;161:3596–606.
15. Zeng G, Li Y, El-Gamil M, *et al*. Generation of NY-ESO-1-specific CD4+ and CD8+ T cells by a single peptide with dual MHC class I and class II specificities: a new strategy for vaccine design. *Cancer Res* 2002;62:3630–5.
16. Zeng G, Touloukian CE, Wang X, *et al*. Identification of CD4+ T cell epitopes from NY-ESO-1 presented by HLA-DR molecules. *J Immunol* 2000;165:1153–9.
17. Zeng G, Wang X, Robbins PF, *et al*. CD4(+) T cell recognition of MHC class II-restricted epitopes from NY-ESO-1 presented by a prevalent HLA DP4 allele: association with NY-ESO-1 antibody production. *Proc Natl Acad Sci U S A* 2001;98:3964–9.
18. Wang RF, Rosenberg SA. Human tumor antigens for cancer vaccine development. *Immunol Rev* 1999;170:85–100.
19. Jäger E, Chen YT, Drijfhout JW, *et al*. Simultaneous humoral and cellular immune response against cancer-testis antigen NY-ESO-1: definition of human histocompatibility leukocyte antigen (HLA)-A2-binding peptide epitopes. *J Exp Med* 1998;187:265–70.
20. Stockert E, Jäger E, Chen YT, *et al*. A survey of the humoral immune response of cancer patients to a panel of human tumor antigens. *J Exp Med* 1998;187:1349–54.
21. Lee L, Wang R-F, Wang X, *et al*. NY-ESO-1 may be a potential target for lung cancer immunotherapy. *Cancer J Sci Am* 1999;5:20–5.
22. Robbins PF, Morgan RA, Feldman SA, *et al*. Tumor regression in patients with metastatic synovial cell sarcoma and melanoma using genetically engineered lymphocytes reactive with NY-ESO-1. *J Clin Oncol* 2011;29:917–24.
23. Robbins PF, Kassim SH, Tran TLN, *et al*. A pilot trial using lymphocytes genetically engineered with an NY-ESO-1-reactive T-cell receptor: long-term follow-up and correlates with response. *Clin Cancer Res* 2015;21:1019–27.
24. Rapoport AP, Stadtmauer EA, Binder-Scholl GK. NY-ESO-1-specific TCR-engineered T cells mediate sustained antigen-specific antitumor effects in myeloma. *Nat Med 2015;Published online* 2015;21:914–21.
25. Dao T, Yan S, Veomett N, *et al*. Targeting the intracellular WT1 oncogene product with a therapeutic human antibody. *Sci Transl Med* 2013;5:176ra33.
26. Sergeeva A, He H, Ruisaard K, *et al*. Activity of 8F4, a T-cell receptor-like anti-PR1/HLA-A2 antibody, against primary human AML in vivo. *Leukemia* 2016;30:1475–84.
27. Dahan R, Reiter Y. T-cell-receptor-like antibodies - generation, function and applications. *Expert Rev Mol Med* 2012;14:e6.
28. Dao T, Pankov D, Scott A, *et al*. Therapeutic bispecific T-cell engager antibody targeting the intracellular oncoprotein WT1. *Nat Biotechnol* 2015;33:1079–86.
29. Ma Q, Garber HR, Lu S, *et al*. A novel TCR-like CAR with specificity for PR1/HLA-A2 effectively targets myeloid leukemia in vitro when expressed in human adult peripheral blood and cord blood T cells. *Cytotherapy* 2016;18:985–94.
30. Rafiq S, Purdon TJ, Daniyan AF, *et al*. Optimized T-cell receptor-mimic chimeric antigen receptor T cells directed toward the intracellular Wilms tumor 1 antigen. *Leukemia* 2017;31:1788–97.
31. Lowe DB, Bivens CK, Mobley AS, *et al*. TCR-like antibody drug conjugates mediate killing of tumor cells with low peptide/HLA targets. *MAbs* 2017;9:603–14.
32. Lai J, Wang Y, Wu S-S, *et al*. Elimination of melanoma by sortase A-generated TCR-like antibody-drug conjugates (TL-ADCs) targeting intracellular melanoma antigen MART-1. *Biomaterials* 2018;178:158–69.
33. Xie G, Ivica NA, Jia B, *et al*. CAR-T cells targeting a nucleophosmin neoepitope exhibit potent specific activity in mouse models of acute myeloid leukaemia. *Nat Biomed Eng* 2021;5:399–413.
34. Ku Z, Xie X, Davidson E, *et al*. Molecular determinants and mechanism for antibody cocktail preventing SARS-CoV-2 escape. *Nat Commun* 2021;12:469.
35. Held G, Matsuo M, Epel M, *et al*. Dissecting cytotoxic T cell responses towards the NY-ESO-1 protein by peptide/MHC-specific antibody fragments. *Eur J Immunol* 2004;34:2919–29.

36 Stewart-Jones G, Wadle A, Hombach A, *et al*. Rational development of high-affinity T-cell receptor-like antibodies. *Proc Natl Acad Sci U S A* 2009;106:5784–8.

37 Maus MV, Plotkin J, Jakka G, *et al*. An MHC-restricted antibody-based chimeric antigen receptor requires TCR-like affinity to maintain antigen specificity. *Mol Ther Oncolytics* 2016;3:1–9.

38 Holler PD, Chlewicki LK, Kranz DM. TCRs with high affinity for foreign pMHC show self-reactivity. *Nat Immunol* 2003;4:55–62.

39 Weber KS, Donermeyer DL, Allen PM, *et al*. Class II-restricted T cell receptor engineered in vitro for higher affinity retains peptide specificity and function. *Proc Natl Acad Sci U S A* 2005;102:19033–8.

40 Zhao Y, Bennett AD, Zheng Z, *et al*. High-affinity TCRs generated by phage display provide CD4+ T cells with the ability to recognize and kill tumor cell lines. *J Immunol* 2007;179:5845–54.

41 Li Y, Moysey R, Molloy PE, *et al*. Directed evolution of human T-cell receptors with picomolar affinities by phage display. *Nat Biotechnol* 2005;23:349–54.

42 Inaguma Y, Akahori Y, Murayama Y, *et al*. Construction and molecular characterization of a T-cell receptor-like antibody and CAR-T cells specific for minor histocompatibility antigen HA-1H. *Gene Ther* 2014;21:575–84.

43 Oren R, Hod-Marco M, Haus-Cohen M, *et al*. Functional comparison of engineered T cells carrying a native TCR versus TCR-like antibody-based chimeric antigen receptors indicates affinity/avidity thresholds. *J Immunol* 2014;193:5733–43.

44 Robbins PF, Li YF, El-Gamil M, *et al*. Single and dual amino acid substitutions in TCR CDRs can enhance antigen-specific T cell functions. *J Immunol* 2008;180:6116–31.

45 Watanabe K, Terakura S, Martens AC, *et al*. Target antigen density governs the efficacy of anti-CD20-CD28-CD3 ζ chimeric antigen receptor-modified effector CD8+ T cells. *J Immunol* 2015;194:911–20.

46 Akatsuka Y. TCR-Like CAR-T cells targeting MHC-Bound minor histocompatibility antigens. *Front Immunol* 2020;11:257.

47 Adachi K, Kano Y, Nagai T, *et al*. Il-7 and CCL19 expression in CAR-T cells improves immune cell infiltration and CAR-T cell survival in the tumor. *Nat Biotechnol* 2018;36:346–51.

48 Waldman AD, Fritz JM, Lenardo MJ. A guide to cancer immunotherapy: from T cell basic science to clinical practice. *Nat Rev Immunol* 2020;20:651–68.

49 Mikucki ME, Fisher DT, Matsuzaki J, *et al*. Non-redundant requirement for CXCR3 signalling during tumoricidal T-cell trafficking across tumour vascular checkpoints. *Nat Commun* 2015;6:7458.